

RESEARCH ARTICLE

10.1002/2014WR016237

On the control of riverbed incision induced by run-of-river power plant

Simone Bizzi¹, Quang Dinh², Dario Bernardi³, Simona Denaro², Leonardo Schippa³, and Rodolfo Soncini-Sessa²

Key Points:

- Riverbed degradation included in MO optimization of reservoir operation
- Surrogate modeling of a hydro-morphological model by response surface
- Pareto-optimal solutions derived for hydropower revenue and riverbed incision

¹European Commission, Joint Research Centre (JRC), Institute for Environment and Sustainability (IES), Water Resources Unit, Ispra (VA), Italy, ²Department of Electronics, Information, and Bioengineering, Politecnico di Milano, Milano, Italy, ³Engineering Department, University of Ferrara, Ferrara, Italy

Correspondence to:

S. Bizzi,
simone.bizzi@jrc.ec.europa.eu

Citation:

Bizzi, S., Q. Dinh, D. Bernardi, S. Denaro, L. Schippa, and R. Soncini-Sessa (2015), On the control of riverbed incision induced by run-of-river power plant, *Water Resour. Res.*, 51, 5023–5040, doi:10.1002/2014WR016237.

Received 2 AUG 2014

Accepted 29 MAY 2015

Accepted article online 1 JUN 2015

Published online 2 JUL 2015

The copyright line for this article was changed on 29 FEB 2016 after original online publication.

Abstract Water resource management (WRM) through dams or reservoirs is worldwide necessary to support key human-related activities, ranging from hydropower production to water allocation and flood risk mitigation. Designing of reservoir operations aims primarily to fulfill the main purpose (or purposes) for which the structure has been built. However, it is well known that reservoirs strongly influence river geomorphic processes, causing sediment deficits downstream, altering water, and sediment fluxes, leading to riverbed incision and causing infrastructure instability and ecological degradation. We propose a framework that, by combining physically based modeling, surrogate modeling techniques, and multiobjective (MO) optimization, allows to include fluvial geomorphology into MO optimization whose main objectives are the maximization of hydropower revenue and the minimization of riverbed degradation. The case study is a run-of-the-river power plant on the River Po (Italy). A 1-D mobile-bed hydro-morphological model simulated the riverbed evolution over a 10 year horizon for alternatives operation rules of the power plant. The knowledge provided by such a physically based model is integrated into a MO optimization routine via surrogate modeling using the response surface methodology. Hence, this framework overcomes the high computational costs that so far hindered the integration of river geomorphology into WRM. We provided numerical proof that river morphologic processes and hydropower production are indeed in conflict but that the conflict may be mitigated with appropriate control strategies.

1. Introduction

Dams and reservoirs are essential for many human-related activities involving water management. Their purposes range from water allocation for irrigation, industrial and domestic supply to hydropower production, flood risk mitigation, land reclamation, and recreation. Regardless of their purpose, reservoirs affect the longitudinal continuity of fluvial water and sediment flow and alter the flood peaks and seasonal distribution of discharges causing substantial geomorphological adjustment downstream [Kondolf, 1997].

A vast amount of literature has studied the effects of dams on river systems in terms of both geomorphological and ecological responses [Poff and Hart, 2002; Gupta et al., 2012; Petts and Gurnell, 2005]. Dams affect the hydrological regime downstream primarily through changes in timing, magnitude, and frequency of high and low flows [Magilligan and Nislow, 2005]. Peak discharge downstream is generally significantly reduced. Sediment connectivity is altered by dams which trap a large amount of sediment load delivered from upstream. In response to the altered water and sediment fluxes, channel aims to establish a new equilibrium by a complex range of geomorphological adjustments which can include several steps and may take decades before reaching a more stable condition [Petts and Gurnell, 2005]. Channel changes can include alterations of the cross section, bed material (e.g., coarsening), slope, pattern, and bed forms. By trapping sediment upstream, reservoirs can often cause the river transport capacity to exceed the available sediment supply, creating a sediment deficit downstream [Grant et al., 2003], which in turn triggers river erosion both on the riverbed and the banks. This process can extend over hundreds of kilometers and last for decades.

Some frameworks have been developed to assess the effects of sediment trapping of dams on river channel processes [Grant et al., 2003; Burke et al., 2009]. Nevertheless, when planning dam operation rules only the

© 2015. The Authors.

This is an open access article under the terms of the Creative Commons Attribution-NonCommercial-NoDerivs License, which permits use and distribution in any medium, provided the original work is properly cited, the use is non-commercial and no modifications or adaptations are made.

fulfillment of the main purpose (or purposes) for which the structure has been built is considered, often hydropower production or water supply. Few studies included the influences of dam operations on river processes [Wild and Loucks, 2014; Yin et al., 2014].

Multiobjective (MO) approaches can take into account a variety of societal needs affected by the dam management from flood mitigation to water supply or environmental quality. MO methods have been adopted to provide decision makers and stakeholders with valuable tools to evaluate the consequences of alternative operating rules from a variety of perspectives [Castelletti et al., 2007; Yin et al., 2009]. These experiences have marked a significant progress in our ability to plan sustainable management of water resources and provided more comprehensive insights into how dams affect the fluvial system and the related ecosystem services. However, integration of fluvial geomorphological process into the planning of optimal operating rules remains very rare. Some authors implicitly addressed the issue by managing flashing floods to restore basic environmental functions [Dittmann et al., 2009; Wu and Chou, 2004; Gómez et al., 2013; Yin et al., 2014]. More recently, Wild and Loucks [2014] addressed similar issues at catchment scale, assessing the cascade effects of multiple dams in the Mekong basin on sediment connectivity. With the exception of a single example [Nicklow and Mays, 2000; Nicklow and Ozkurt, 2003], studies that have optimized dam regulations in order to minimize their impact on channel morphological adjustments downstream are absent. Nevertheless, the operational value of this previous approach was limited. The model relied on a single-objective framework, i.e., considered the effect of operating rules on downstream riverbed incision, but neglected other objectives such as hydropower revenue or water supply as commonly addressed in a MO approach. Additionally, the framework did not provide daily operation rules, but focused on flood conditions, only.

The lack of consideration of river geomorphology in MO water management in the scientific community is surprising, considering the recent interest for multiple, negative effects of dams on channel morphodynamics. One reason is in the currently limited capability for predicting fluvial geomorphological response on the relevant time scales [Brasington and Richards, 2007]. On the other hand, channel morphological alterations develop over time scales from decades to centuries, and many of these alterations were not foreseeable during the second half of the last century, when most of the dams have been built worldwide. Finally, it is unclear to what extent optimal operating rules accounting for fluvial geomorphology can reduce negative morphological effects.

Nowadays, running physically based (PB) models that simulate both hydrodynamics and riverbed evolution over extended spatiotemporal scales are feasible due to increased computer power [Langendoen et al., 2009]. These models could be suitable to derive detailed estimates of river morphological response to dam construction and regulation. Unfortunately, the computational costs of such a procedure are still too high to allow for integration into MO optimization routines. MO optimization routines need to evaluate an elevated number of different alternatives in order to identify the Pareto-optimal decisions [Castelletti et al., 2007]. The high number of required model evaluations makes the integration of PB river evolution models into MO optimization practically infeasible. Nevertheless, the computational burden associated to PB models ranging from water quality to water distribution issues [see Razavi et al., 2012, and reference therein] is a common problem in MO water management. To overcome this limitation, PB models can be replaced by surrogate models that maintain key characteristics of the original model, but require only a fraction of computational effort. A range of surrogate models has been developed over the past decades, and are now widely applied [Razavi et al., 2012; Castelletti et al., 2012].

The aim of this contribution is to propose a modeling methodology of general validity for including riverbed degradation when designing optimal operating rules of reservoirs. Specific goals of this research are (i) testing the suitability of surrogate modeling, such as global Response Surface Methodology (RSM), to integrate a 1-D PB hydro-morphological model into a MO design problem to identify Pareto-optimal operating rules of a HP plant; (ii) assessing the feasibility and utility to account for the river geomorphic changes when planning optimal operating rules.

This paper analyzes the effect of alternative operating rules for Isola Serafini—a run-of-river HP plant on the River Po, Italy—where the downstream river reach is affected by a severe incision rate since 1960s. We implemented a one-dimensional PB hydro-morphological model to simulate the riverbed evolution over a time horizon of 10 years along a 112 km long river stretch. We then built a MO framework to assess the effects of alternative operating rules on hydropower revenue and riverbed incision, and finally provide

Pareto-optimal decision rules. We adopted the global RSM [Castelletti *et al.*, 2010a] as surrogate modeling technique to embed the PB hydro-morphological model into the MO optimization framework.

We start from the case study description, and the introduction to the hydro-morphological model to facilitate the following description of the control problem. The MO control problem is formulated and the main aspects of the (global) RSM are briefly recalled. Two alternative control schemes are proposed: a pure feedforward control scheme (Scheme A) and a mixed feedforward-feedback control scheme (Scheme B). They are implemented for the case study and their performance is analyzed. We conclude with a discussion of potentials and limits of the proposed framework for future applications.

2. The Case Study: The River Po and the Isola Serafini HP Plant

The case study of Isola Serafini (IS) run-of-river hydro-power-plant (HPP) in the Po valley (Italy) is presented in Figure 1. The Po is the longest river in Italy and runs for 652 km across the northern regions from the Alps to the Adriatic Sea, with a catchment area of approximately 70,000 km². The River Po is widely exploited, most of all as a source for irrigation in the fertile valley, but also as an important waterway. The present study focuses on a 112 km reach (see Figure 1) from Piacenza to Boretto, which includes the IS HPP.

The power plant (Figure 1) is located 30 km downstream of Piacenza and has been operating since 1962. It consists of a barrage which diverts part of the incoming flow to four vertical Kaplan turbines (total installed power capacity 80 MW). The diversion channel was originally the result of a meander cutoff during the large 1951 flood and joins the main channel 12 km downstream of the diversion (Figure 1). The barrage has 11 sluice gates of equal width. Two gates feature a lowered bottom for sediment-scouring purposes. Six gates can be overtopped functioning as sharp-crested weirs. There is no room for water storage behind the barrage, except for short transitories during maneuvers, pondage is not a management option.

During the twentieth century, the middle-lower course of River Po has experienced a significant degradation of the bed, a process that accelerated after the construction of IS HPP, which altered the flow regime and created a sediment transport disconnection. There are also other human pressures affecting both sediment supply and sediment transport capacity. Among these, instream sand mining seems to be very relevant. Sand mining was very intense from 1950 until 1980. After that, stricter regulations have first reduced and then stopped the activity. Surian and Rinaldi [2003] state that instream mining increased from about 3 to 12 million m³/yr in the period 1960–1980, and then decreased to about 4 million m³/yr. The peak volume (12 million m³/yr) is estimated to be not far from the assessed average annual sediment yield of the basin.

As consequence of riverbed lowering, several navigation and irrigation structures became unusable during low flow periods, e.g., harbor locks in Cremona, where minimum water levels decreased by more than 4 m from 1950 to 2000 requiring expensive interventions to rebuild locks or restore their functionality. The estimated costs of the new locks alone exceed € 40 millions [Bonomo and Luisa, 2011]. Other impacts include instability of, e.g., flood protections and infrastructures, and freshwater ecological alterations, for which economical appraisals are missing.

For all these reasons, IS HPP is a challenging case study to assess optimal operating rules that maximize hydropower revenue and minimize riverbed incision downstream of the plant. In particular, we analyze the effects of alternative operating rules over a time horizon of 10 years in terms of riverbed incision nearby Cremona. This reach has been significantly affected by riverbed degradation in the past and has a strategic role for navigation and flood defense. Our choice is also supported by the findings of Bernardi *et al.* [2013], which have shown that this reach is the most sensitive to IS operation. Toward this aim, we refer to a complete historical time series of water inflows from 1964 to 1973 recorded at Piacenza, and at the relevant tributaries. For this period, data are readily available and are suitable for this illustrative case study.

3. Modeling the System

3.1. Isola Serafini Operating Rules

The only objective of the IS HPP is electricity generation: its present operating rule aims at maximizing hydropower production. The water level upstream the dam is constantly kept at 41.00 m a.s.l. with a

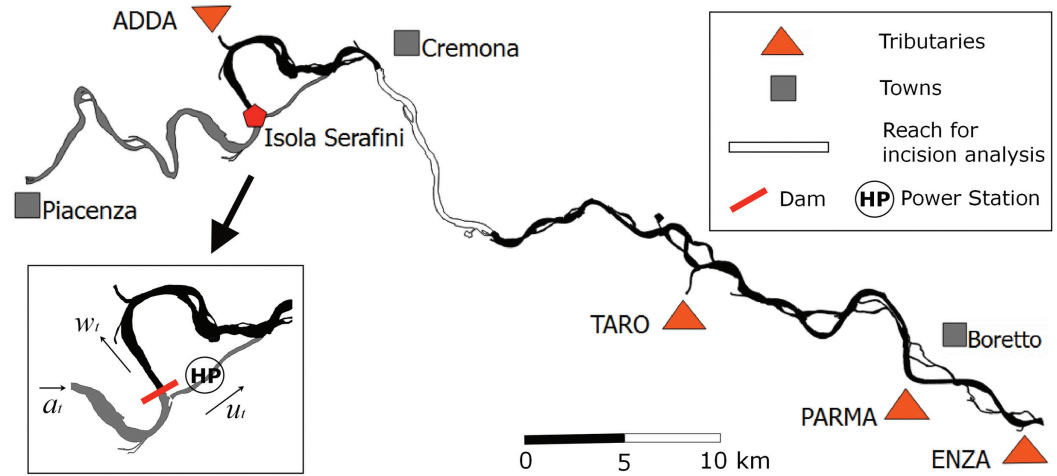


Figure 1. Scheme of the Isola Serafini and the stretch of the River Po analyzed.

maximum tolerance of 0.50 m. The production is stopped during floods for safety reasons. As previously recalled, no water pondage is allowed so continuity at the bifurcation is satisfied at any time.

The IS operating rule-curve is shown in Figure 2. A Minimum Environmental Flow (MEF) of 100 m³/s is imposed, and the minimum design flow of the turbines is 200 m³/s. Hence, if the incoming flow a is lower than 300 m³/s the turbined flow u is null, whereas when a is greater than 300 m³/s, all inflow exceeding the MEF is diverted to the turbines until the plant capacity (1000 m³/s) is reached. For larger values of the inflow a , the power station keeps working at its maximum capacity and all the additional discharge passes throughout the gates and flows into the meander. When the incoming flow a exceeds 4000 m³/s the turbines stop working (u is set to zero) for safety reason, and to avoid upstream flooding, all the gates are fully opened to allow flood pass-through.

For designing the new operating rules, we consider the following class of piecewise linear operating rules such as the one defined by the bold black line in Figure 3:

$$\begin{cases} u=0 & \text{if } 0 \leq a \leq 200+MEF \\ u=\min(a-MEF, 1000) & \text{if } 200+MEF < a \leq \theta_1 \\ u=\min(\theta_2+\theta_3 \cdot (a-\theta_1), 1000) & \text{if } \theta_1 < a \leq \theta_4 \\ u=0 & \text{if } a > \theta_4 \end{cases} \quad (1)$$

A specific rule within this class is defined by instantiating a four-dimensional design parameter vector θ , the four elements of which are denoted as $\theta_1, \theta_2, \theta_3$, and θ_4 . The parameter θ_4 is the discharge threshold at which all the gates of the barrage are completely open. It primarily affects sediment supply to the downstream reach through the gates, while the other three parameters affect the transport capacity in the meander by reducing the discharge u through the turbines.

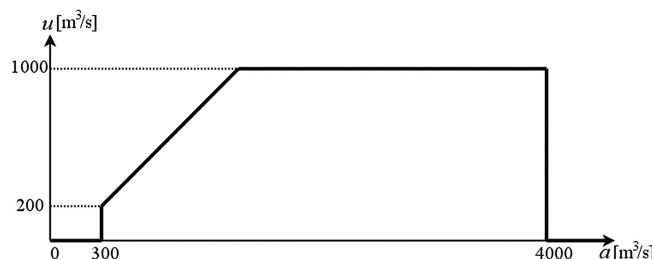


Figure 2. Present Isola Serafini operating rule.

The present operating rule (in the following named Business As Usual-BAU-rule) is a particular rule of this class and can be obtained by alternative instantiations of the parameters, for instance,

$$\theta_1 \geq 300, \theta_2=1000, \theta_3=0, \theta_4=4000. \quad (2)$$

The vector θ should be chosen within a feasible domain which can be extracted from the current operating

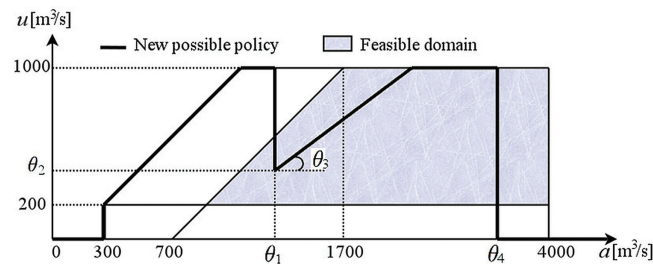


Figure 3. The gray area is the feasible domain defined by equations (1) and (3), within which alternative operating rules can be designed. A specific rule (bold black line) is specified by instantiating the four parameters θ_1 , θ_2 , θ_3 , and θ_4 .

rule, since it accounts for the physical constraints: the MEF, the minimum and maximum flow through the turbines, and the safety limit against flood risk. Moreover, previous studies on the Po River have shown that the sediment transport in the meander is triggered only when the discharge is larger than 700 m³/s [Rosatti et al., 2008]. Taking care of all these conditions, the feasible set Θ (see also equation (13d)) is specified by

$$\begin{cases} 2000 < \theta_4 \leq 4000 \\ 900 < \theta_1 \leq \theta_4 \\ 200 < \theta_2 \leq \min(\theta_1 - 700, 1000) \\ 0 < \theta_3 \leq 1 \end{cases}, \quad (3)$$

and the corresponding operating rules lies within the gray area in Figure 3.

3.2. The Hydro-Morphological Model

To represent the riverbed evolution processes correctly at the reach scale over a 10 year horizon, and to avoid excessive computational times the choice fell on a one-dimensional mobile bed hydro-morphological model. The model was first introduced in a previous work by Schippa et al. [2006]. We adopted the version of the model presented in Schippa and Pavan [2009], and adapted it to the specific requirements of the case study.

The model is based on a set of three differential equations, namely, the shallow water equations for discharge mass balance (see equation (4a)), the momentum balance (see equation (4b)) of the liquid phase, and the Exner equation for the mass balance of the solid phase (see equation (4c))

$$\frac{\partial A}{\partial t} + \frac{\partial Q}{\partial x} = q, \quad (4a)$$

$$\frac{\partial Q}{\partial x} + \frac{\partial}{\partial x} \left(\frac{Q^2}{A} + gI_1 \right) = \frac{\partial I_1}{\partial x} \Big|_{z_w} - gAS_f, \quad (4b)$$

$$(1-p) \frac{\partial A_b}{\partial t} + \frac{\partial Q_s}{\partial x} = q_s. \quad (4c)$$

Here t is the time, x is the longitudinal stream coordinate, A is the cross-section wetted area, Q is the liquid discharge, g is the gravity acceleration, I_1 is the static moment of the wetted area A with respect to the water surface, S_f is the friction slope, A_b is the sediment volume per unit length of the stream subject to erosion or deposition (sediment area), Q_s is the solid discharge, q and q_s are the liquid and solid lateral inflows (or outflows) per unit length, respectively (see Figure 4).

The first term in the right-hand side of equation (4b) represents the variation of the static moment I_1 along the x coordinate at a constant water level z_w [Capart et al., 2003; Schippa and Pavan, 2008]. This formulation avoids an undesirable explicit definition of the local bed slope in the momentum balance equation that often leads to incorrect momentum balance in natural rivers.

To complete the equations system, two closure equations have been used, i.e., Manning formula [Manning, 1891] for computing the friction slope, and Engelund-Hansen formula [Engelund and Hansen, 1967], for computing total sediment transport (bed load and suspended load together). The latter has been tested and compared to other sediment transport formulas during previous extensive studies on the Po river

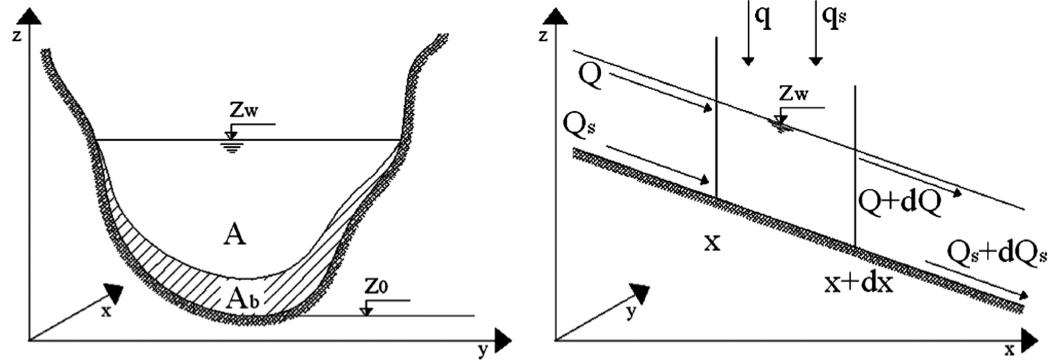


Figure 4. Cross-section scheme and variable definition for the hydro-morphological model.

[Ministero delle Politiche Agricole Alimentari e Forestali, 1990], and was representing sediment movement in this reach well.

As for the sediment mass balance, the solution of equation (4c) updates the value of A_b at every time step. For every wetted point of the cross section, the variation of this value has to be converted into an elevation difference, Δs . It is assumed that Δs is proportional to bed shear stress, and consequently to local water depth h through a constant k :

$$\Delta s = kh. \tag{5}$$

The variation of sediment area ΔA_b , at every time step, is obtained by integration of Δs along the wetted perimeter P

$$\int_P \Delta s dp = \Delta A_b. \tag{6}$$

The same integration on the right-hand side of equation (5) leads to the wetted area A . Therefore, k is known and the local bed variation due to erosion or deposition is computed directly via equation (5).

To integrate equation (4), the finite difference explicit scheme developed by McCormack was chosen, for its easy implementation and its ability to cope with discontinuities in the solution.

The river stretch is split in two substretches: the first is from Piacenza to IS dam (30 km) and the second from IS dam to Boretto (82 km) (Figure 1). In a field campaign in 2009, the Interregional Po Agency (AIPO) surveyed 67 cross sections in the two substretches, with an average spacing of 1.69 km. For every cross section survey, the boundary of the overbanks and the thalweg was identified. In the model simulations the interdistance between the cross sections is reduced. Therefore, additional cross sections are derived by linear interpolation from measurements, to reach a distance of 450 m between cross sections. This increased the number of cross sections along the reach to 250. Roughness coefficients were calibrated during previous studies [Schippa et al., 2006].

The hydrodynamic boundary conditions at Piacenza and Boretto (historical discharge data and the stage-discharge function) are extracted from regional environment agencies bulletins. Four tributaries join the river in stretch 2. The power station channel joins the river between the Adda river confluence and Cremona. When the HP plant is operating, the two stretches 1 and 2 are disconnected: for stretch 1, the downstream boundary condition is the imposed water level, whereas the operating rule of the gate provides the upstream boundary conditions for stretch 2, both in terms of liquid (w) and solid discharges $Q_s^{str2,up}$. Modeling the sediment transport in proximity of the barrage requires some assumptions. When the power station is operating and the gates are at least partially closed, $Q_s^{str2,up}$ is calculated as follows:

$$Q_s^{str2,up} = Q_s^{str1,down} * 0.7 * \left(\frac{W}{a}\right)^{1.7}, \tag{7}$$

where $Q_s^{str1,down}$ is the sediment discharge approaching IS.

The empirical reduction coefficient 0.7 is applied to take into account the fact that not all of the eleven gates are necessarily open when the HPP is operating, so part of the sediment is retained. Anyway, it should be noticed that when power station is operating, water velocity and transport capacity upstream of the barrage are small.

When the discharge is above the safety limit, instead, all the gates are fully open instead. No flow is diverted to the power plant channel ($u = 0$) and the two reaches 1 and 2 are linked. With all gates open, we may assume that full continuity is satisfied also for sediment transport, since most part of the sediment moves by saltation-suspension and not by traction close to the bed [Ministero delle Politiche Agricole Alimentari e Forestali, 1990].

4. Defining the Objectives

Two conflicting objectives are considered: the hydropower revenue and the incision rate in the reach under study (white line in Figure 1).

The expected yearly hydropower revenue J^{hp} [€/year] is the cumulated value of daily revenue over the evaluated time horizon (of n days) divided by the number N of years in the same horizon; the daily revenue is the product of the daily hydropower energy production (P_t) by the time-varying energy unit price π_t (€/kW), i.e.,

$$J^{hp} = \frac{1}{N} \sum_{t=1}^n \pi_t P_t, \tag{8}$$

where n is the number of days and N the number of years in the evaluation horizon.

The hydropower production P_t (kW) is a function of the turbined release u_t , the head jump H_t , and the turbine efficiency $\eta(H_t)$, which in turn depends on the head jump. That is,

$$P_t = \varphi g \rho \eta_t u_t H_t, \tag{9}$$

where φ is a coefficient for dimensional conversion, g is the gravitational acceleration (9.81 m/s^2), and ρ is the water density (1000 kg/m^3).

The hydraulic head is the difference between the water level upstream the gate (h_t^{up}) and the water level just downstream the turbines (h_t^{down}):

$$H_t = h_t^{up} - h_t^{down}. \tag{10}$$

Since the flow profile in the power station channel is not computed by the hydro-morphological model, h^{down} is assumed to be given by an empirical relationship: $h^{down} = f(u, h^{junc})$, where h^{junc} is the water level at the junction between the power plant channel and the River Po, which is computed by the hydro-morphological model.

To quantify erosion we monitor the evolution of the bed level at five prespecified points within each cross section. The first point is the *thalweg*, and two other points are selected on the left and on the right side of the bed in each of M cross sections. Let us denote with $z_{ij}^b(y)$ the bed level in the i th point ($i = 1, \dots, 5$) of the j th cross section ($j = 1, \dots, M$) at the first day of the y th year of the evaluation horizon. The bed level change i_y in the reach under study at the beginning of the y th year is defined as the average difference of level between the starting of the evaluation horizon and that instant all over the sampled points, i.e.,

$$i_y = \frac{1}{5M} \sum_{i=1}^5 \sum_{j=1}^M (z_{ij}^b(y) - z_{ij}^b(0)). \tag{11}$$

To quantify incision resulting from any operating rule we consider the expected yearly incision rate over the evaluation horizon, i.e., we adopt as incision indicator J^{inc} (m/yr) such that

$$J^{inc} = i_N / N, \tag{12}$$

where N is the number of years in the evaluation horizon (in the study we consider 10 years).

A negative j^{inc} indicates degradation. All variables needed for the calculation of the two objectives result from the hydro-morphological model. Both the objectives, j^{hp} and j^{inc} have to be maximized.

5. Problem Formulation and Solution Procedure

The MO design problem for IS can thus be formulated

$$\min_{\theta} J(\mathbf{x}_0^{h-1}, u_0^{h-1}, a_1^h), \tag{13a}$$

subject to

$$\mathbf{x}_{t+1} = f_t(\mathbf{x}_t, u_t, a_{t+1}) \quad t=0, 1, \dots, h-1, \tag{13b}$$

$$u_t = m_t(a_t, \theta) \quad t=0, 1, \dots, h, \tag{13c}$$

$$\theta \in \Theta, \tag{13d}$$

$$a_1^h \text{ given inflow scenario}, \tag{13e}$$

$$\mathbf{x}_0 = \bar{\mathbf{x}}_0. \tag{13f}$$

a_t is the incoming flow, u_t is the flow diverted to the HPP, and w_t is the discharge that flows to the meander through the gates of the barrage (see Figure 1). The flow u_t is led back into the main channel few kilometers downstream. This is an established formulation for MO problems in water resources [Soncini-Sessa et al., 2007]. The target is to identify optimal operating rules $m(\cdot)$ that determine the diverted flow u_t as a function of the incoming flow a_t and the design parameter vector θ . The operating rules must be pareto-optimal in the sense that they maximize the management objectives j^{hp} and j^{inc} . The hydro-morphological model component is represented in the control law by $\mathbf{x}_{t+1} = f_t(\mathbf{x}_t, u_t, a_{t+1})$. It is a lumped spatially distributed dynamic model capable of producing the necessary information related to water and riverbed levels (the vector of states \mathbf{x}) to calculate the objective vectors \mathbf{J} . The objectives for this case study $j^{inc}(\mathbf{x}_0^{h-1}, u_0^{h-1}, a_1^h)$, $j^{hp}(\mathbf{x}_0^{h-1}, u_0^{h-1}, a_1^h)$ condense the information provided by the hydro-morphological model via time and space aggregation, in correspondence of a given evaluation inflow scenario (a_1^h) [Soncini-Sessa et al., 2007].

The solution of Problem (13) requires thousands of evaluation of the hydro-morphological model. Ten years of simulation of the analyzed river stretch is run in approximately 1 day in a 3.4 GHz quad-core desktop computer. This makes direct computation of the objectives computationally demanding and hardly solvable within useful computational time. Hence, surrogate modeling techniques can be used to reduce the computational burden. In the following section we introduce the response surface methodology that was selected as a surrogate model in this case study.

5.1. Response Surface Methodology

A wide variety of surrogate models have been developed over the past decades and their use is becoming more and more popular within the water resources community [Razavi et al., 2012]. The Response Surface Methodology (RSM) was first proposed by Box and Wilson [1951] and was widely implemented both for single-objective and MO optimization [Kleijnen, 2008].

In this case study we adopt the *Learning and Planning RS* (LP-RS) procedure proposed by [Castelletti et al., 2010a], to solve the MO design problem using a global interactive response surface methodology. Technical introductions to this method can be found in Castelletti et al. [2010a] and reference therein. Here we provide some basic principles of the LP-RS procedure. Appendix A introduces some more technical details in order to support future applications.

A classical optimization algorithm for solving the design problem (13) evolves in the space of the design parameter vector θ and evaluates the corresponding value of the objective \mathbf{J} by simulating the system behavior under a given operation rule. The process ends when the minima of the objectives are found. As noted previously for our case study this approach would require thousands of simulations of the hydro-morphological model. Here is where a global GSM may be of help. Given the problem formulation (13), we are interested to understand the relationships between the objective $\mathbf{J}(\mathbf{x}_0^{h-1}, u_0^{h-1}, a_1^h)$ and the design parameter vector θ . The function $\mathbf{J}(\theta)$, linking objectives and possible operating rules, is named Response

Surface (RS). If the RS function was fully known a priori, it would be possible solve the problem (13) analytically from

$$\min_{\theta \in \Theta} \mathbf{J}(\theta). \tag{14}$$

A complete direct determination of the RS surface is however computationally too expensive since it would require a high number of simulations of the model again. Thus an approximation $\hat{\mathbf{J}}(\theta)$ of the RS is introduced using the LP-RS.

A certain number of appropriate instances of the operating rules (i.e., different values of the design parameter vector θ) are chosen and the corresponding objective values \mathbf{J} are determined via simulation of the hydro-morphological model: the number of instances is a trade-off between the need to properly cover the feasible set of the design parameter vector, and the concern of keeping the simulation time within acceptable limits. At the end of this simulation step, a first training set composed of (θ, \mathbf{J}) couples, is available and is used to identify a first approximation $\hat{\mathbf{J}}^1(\theta)$ of the Response Surface (RS) via interpolation. By assuming that the $\hat{\mathbf{J}}^1(\theta)$ properly represents the RS, the Design Problem 13 is substituted by the following:

$$\min_{\theta \in \Theta} \hat{\mathbf{J}}^1(\theta), \tag{15}$$

whose solution, the Pareto front in the space \mathbf{J} , is straightforward. The solution of Problem 15 is the last step of the first iteration of the LP-RS procedure.

In order to check whether the approximation $\hat{\mathbf{J}}^1(\theta)$ of the RS is adequate, a few operating rules (i.e., a few values of the design parameter vector) are selected on the Pareto front and simulated via the PB model. These new simulations increase the number of couples (θ, \mathbf{J}) in the training set. With them an updated approximation $\hat{\mathbf{J}}^2(\theta)$ of the RS is identified and substituted instead of $\hat{\mathbf{J}}^1(\theta)$ in Problem 15. The new Problem is solved and an updated Pareto front is obtained. This concludes the second iteration of the procedure. As in the second iteration, the third one also starts by choosing few points on the new Pareto front.

After the second and each following iteration, a termination test is performed to determine when to stop the procedure. We based our criteria on the RS accuracy. It considers the distances e^j between the values of the j th objective obtained via PB model simulation and the ones given by the RS approximation at the previous iteration. If the average distance \bar{e}^j is below a given tolerance λ^j , the Pareto front based on the approximated RS is considered a good approximation of the PB model itself, and the procedure is terminated. Otherwise, a further iteration is performed. The thresholds λ^j have to be set by the designer [Wang et al., 2001]: their values are chosen according to the type of problem and the adopted objectives. Once more, the goal is to find the right compromise between the desired accuracy, and the available computational power. In our case, the termination test verifies that the average distance \bar{e}^j is only a small part of the range R^j within which each objective J_j , computed by the RS approximation, can fall. Namely, the threshold λ^j is the 6% of the difference between the maximum and minimum value assumed by the j th objective in the current LP-RS iteration. This means that we assume values of the approximated RS satisfactory as soon as their maximum error is negligible (less than 6%) compare to the range of objective values investigated.

6. Scheme A: Feedforward Control

6.1. Implementation

We consider first a pure *feedforward* control scheme (Figure 5), i.e., an anticipative control law. From a management perspective, this means that at each time t the flow rate a_t entering the reach under study is measured and a release decision u_t is determined according to the operating rule $m^f(\cdot)$ which is defined by the design parameter vector $\theta = [\theta_1, \theta_2, \theta_3, \theta_4]$.

The downstream incision rate could be limited through two different mechanisms: the increase of the sediment supply to the downstream reach, so enhancing sediment connectivity through the barrage, or the increase in discharge and transport capacity to mobilize previously settled sediments. The former is obtained by increasing the number of complete gate openings during medium-high flow events (currently it happens only for flows above 4000 m³/s, see Figure 2), namely by decreasing the threshold θ_4 above

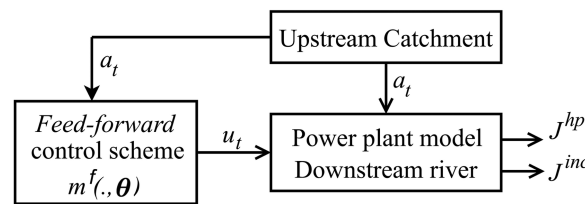


Figure 5. Scheme A— Feedforward control.

which the power plant is turned off. The latter can be accomplished by diverting less water to the power plant. This first scheme (Scheme A) affects both sediment supply and transport capacity.

We started by simulating 49 different instantiations of the vector θ including the BAU alternative. This relatively high number of simulations was necessary to test the

model performance for the case study and to understand the system behavior initially. The main results have been analyzed in Bernardi et al. [2013]. The approximation of the RS can be derived as a function $\hat{J} : \mathcal{R}^4 \rightarrow \mathcal{R}^2$ that describes the relation between the four elements of the vector θ and the corresponding values of the two objectives vector J^{hp} and J^{inc} , then. Identifying the RS approximation is a traditional model identification problem as such it is composed of model selection (fixing the class of the RS), calibration (estimation of the parameters), and model validation, reiterated at each iteration over the updated training set of (θ, \mathbf{J}) couples. We considered five different functional classes: Radial Basis Functions (RBF), Thin-Plate-Splines, Multiquadratic and Cubic and General Regression Neural Networks (GRNN). The model validation is performed with a cross-validation technique [Kohavi et al., 1995]. The training set, obtained via the model simulations, is first normalized and then randomly partitioned into a calibration set and a validation sample set. For each considered class, a RS approximation is identified and the validation mean squared error (MSE) is computed for the validation set. The random partitioning is repeated 10 times. A final MSE is derived as average MSE over the 10 individual validation sets. The function class with the lowest averaged mean squared error in validation is then chosen.

The best interpolators for J^{inc} and J^{hp} are then used to build the first approximation of the two RS, which are evaluated on a discretized approximation of the feasible continuous set Θ , defined by equation (3). The discretization of a continuous multidimensional set can be performed in many ways. Here, we build a hypergrid and sample each grid point as an element of the discretized set Θ . The hypergrid is made of four equally spaced single grids, one for each element of the parameter vector θ . To some extent this method is similar to the latin hypercube sampling [Tang, 1993; Park, 1994]. However, the grid spacing and form is not defined by a statistical law, here. But, it is based upon physical considerations on the system (heuristic method). Table 1 shows the ranges of values for the four element of Θ , the associated step of discretization chosen, and the deriving cardinalities of each element. The cardinality of the discrete set Θ is the product of the cardinalities \mathcal{N}_i of the discretized set of the four parameter of θ and was found to be 68.593 (see Table 1, the combinations that do not satisfy the physical constraints have been removed).

The Pareto dominant solutions are then identified amongst this 68.593 alternatives. Finally the selection of interesting operating rules on the Pareto front to be simulated in the next iteration is performed by an expert (based on visualization techniques, see Lotov et al. [2004]). The procedure is iterated until the termination test is satisfied.

6.2. Results

In the first iteration the 49 couples (θ, \mathbf{J}) are used to identify the best RS interpolation \hat{J} . The best performance is given by the GRNN interpolator for J^{hp} and by the Multiquadratic RBF interpolator for J^{inc} . Therefore, these two interpolators are adopted. On their basis the Pareto-efficient alternatives are then identified and 26 alternatives are identified to be Pareto dominant over 68.593 alternatives. In Figure 6, they are represented by the black dots on the dashed black line (Pareto front). Note that both objectives have to be maximized.

Table 1. Scheme A—Parameter Discretization

Parameter	Range	Step	\mathcal{N}_i
θ_1	900–1700	50	17
θ_2	200–1000	50	17
θ_3	0–1	0.1	11
θ_4	2000–4000	50	41

Interesting alternatives are chosen on the Pareto front, taking care of their physical meaning (the corresponding operating rules). We selected eight interesting alternatives for simulation at the next iteration by the PB hydro-morphological model marked by the blue crosses in Figure 6. The values of the θ elements and the associated objective

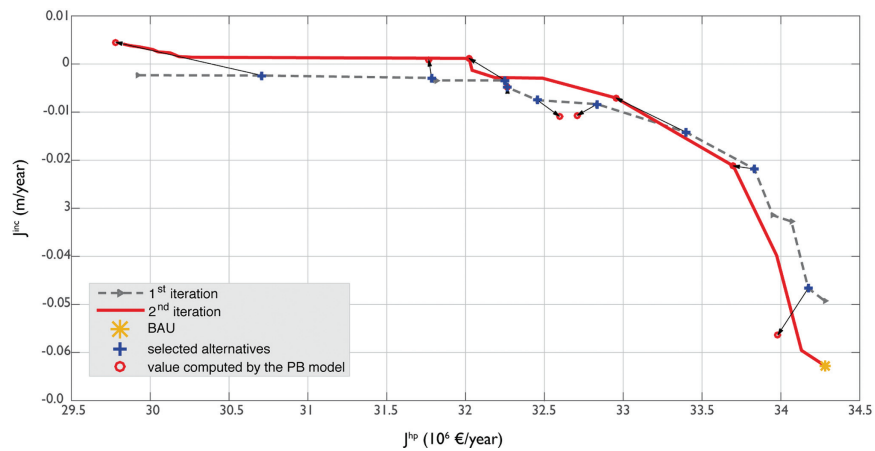


Figure 6. Scheme A—Pareto fronts for first and second iteration. Blue crosses are the alternatives selected on the first Pareto front, red dots the values computed by the hydro-morphological model for those selected alternatives, and the yellow star is the BAU alternative.

values are in Table 2. Red circle points in Figure 6 show the locations of the eight points after the simulation of the hydro-morphological model. The arrows connecting crosses and circles visualize the differences ϵ^j between the approximated objectives (\hat{j}^{hp} and \hat{j}^{inc}) and the simulated ones (J^{hp} and J^{inc}) for those eight alternatives. The eight simulations are added to the previous 49 simulations and used to compute an updated RS approximation. At this second iteration the best fitting is obtained again by the GRNN for both J^{hp} and J^{inc} . These two functional classes are then adopted and, among the 68.593 approximated points of the RS, 42 are identified as Pareto dominant (red line in Figure 6). The procedure stopped here at the second iteration since the termination test is satisfied (see Table 3).

The yellow star plotted on Figure 6 represents the performance of the BAU alternative, i.e., the current operating rule, with an expected hydropower revenue of 34.28 (10^6€) per year and an expected incision rate of -0.0628 m per year. Results coincide with previous studies and call for effective management strategies in the future [Schippa et al., 2006]. The trade-offs inferred from Pareto front indicate that there are several possibilities to reduce the riverbed incision process in the reach considerably with a moderate loss in hydropower revenue.

Both simulated and approximated results reveal a characteristic system response: riverbed evolution is very sensitive to changes of θ_4 . The best performing alternatives (i.e., those with the best J^{hp}/J^{inc} trade-off) are those implementing the current operating rule changing only θ_4 (see Table 2 for details). Conversely, changes in θ_1 , θ_2 , and θ_3 result in substantial reductions in hydropower revenue without significantly affecting incision rate.

A regression analysis was performed to support these findings. A stepwise linear regression is derived from the 57 simulation results to infer the correlations between the components of the

Table 2. Scheme A—Selected Alternatives and Objective Values at the Second Iteration^a

θ_1	θ_2	θ_3	θ_4	\hat{j}^{hp} (10^6 €/yr)	\hat{j}^{inc} (m/yr)	J^{hp} (10^6 €/yr)	J^{inc} (m/yr)	ϵ^{hp} (10^6 €/yr)	ϵ^{inc} (m/yr)
1700	700	0	2000	32.2519	-0.0034	32.0227	0.0012	0.2292	0.0046
1700	850	0	2350	33.3975	-0.0142	32.9547	-0.0071	0.4428	0.0071
1700	350	0.5	2000	31.7857	-0.0030	31.7666	0.0009	0.0191	0.0039
1700	1000	0	2650	33.8320	-0.0218	33.6983	-0.0212	0.1337	0.0006
1700	900	0	3600	34.1736	-0.0466	33.9808	-0.0563	0.1928	0.0097
1700	1000	0	2150	32.8346	-0.0084	32.7085	-0.0107	0.1261	0.0023
1700	1000	0	2100	32.4555	-0.0075	32.5951	-0.0109	0.1396	0.0033
1300	400	0.1	2000	30.7095	-0.0024	29.7821	0.0045	0.9274	0.0069
Average								0.2763	0.0048

^aBAU: $\theta_1 = 1700$, $\theta_2 = 1000$, $\theta_3 = 0$, $\theta_4 = 4000$: $J^{hp} = 34.28$ (10^6 €/yr), $J^{inc} = -0.0628$ (m/yr).

Table 3. Scheme A—Termination Test: The Average Distances \bar{e}^j Are Compared to the Thresholds λ^j (6% of the Ranges R^j)

J^j	R^j	λ^j	\bar{e}^j
\hat{J}^{hp} (10^6 €/yr)	10.9529	0.6571	0.2763
\hat{J}^{inc} (m/yr)	0.0937	0.0056	0.0048

design parameter vector θ and the incision rate J^{inc} . Only the correlation between θ_4 and J^{inc} is statistically significant (see Table 4), which means that re-establishing hydraulic and sediment connectivity during high flow events through a decrease in θ_4 appears to be very effective in contrasting riverbed incision. Based

on these evidences we propose a second scheme (Scheme B) where the value of θ_4 is fixed by a feedback law: this is the subject of the next paragraph.

7. Scheme B

7.1. Implementation

Based on the results of Scheme A, Scheme B combines both *feedforward* and *feedback* control schemes (see Figure 7) together. The system is controlled by a *feedforward* operating rule as in Scheme A. But, at the end of each year y , a *feedback* operating rule $m^b(\cdot)$ modifies the value of the parameter θ_4 of the *feedforward* operating rule and the new value is maintained all over the following year on the base of the registered system output (more precisely the riverbed level variation i_y registered in the previous year). The values of θ_1 , θ_2 , and θ_3 are fixed to the BAU rule. Thus, the parameters of the *feedforward* rule are all defined and the design parameter vector θ is composed of the parameters that specify the *feedback* rule only.

The aim of the control is to keep the yearly rate of riverbed level change i_y/y close to a target value δ (e.g., $\delta = \text{zero}$), i.e., to maintain a constant yearly rate of incision (or deposition). This means that the controller will determine a new value for the parameter θ_4 based on the difference between the observed (i_y) and the target (δy) at the beginning of each year y of simulation. In mathematical terms, in the y th year the value of θ_4 is given by

$$\theta_4 = \alpha + \beta(i_y - \delta y). \tag{16}$$

Equation (16) is the *feedback* rule and α , β , and δ are the three components of the design parameters vector. This means that the RS for \hat{J}^{inc} is a function of α , β , and δ , which is the design parameter vector for Scheme B.

Given a value of δ , the alternatives we are interested in are those for which the *feedback* control law is effective. That means it produces an average yearly incision rate J^{inc} whose value is δ . These alternatives are associated to the intersecting plane between the incision δ and the surface \hat{J}^{inc} in a 4-D space: an exemplification in a 3-D space is reported in Figure 8. Among the alternatives on the intersection plane, only those that maximize the hydropower revenue J^{hp} are Pareto dominant.

Scheme B was tested on few simulation runs in order to determine the most suitable range for each of the new components α , β , and δ of the design parameter vector. As an example, Figure 9 reports the trajectory of incision (J^{inc}) obtained running the hydro-morphological model where θ_4 is produced by equation (16), with α equal to 3700, β equal to 4000, and the targeted incision δ equal to -0.03 (represented as a straight black line in the picture). The ranges of α , β , and δ adopted and their discretization are presented in Table 5. The cardinality of the resulting discretized feasible set Θ is 22,997. On the base of these initial experiments, 25 simulations were used as a basis for starting the iteration cycle of the LP-RS procedure.

7.2. Results and Comparison With Scheme A

For Scheme B four iterations of the LP-RS procedure were necessary to satisfy the termination test (see Table 6), with a total of 58 simulation runs of the hydro-morphological model. Figure 10 shows

Table 4. Regression Analysis: γ Coefficients and p Values

Variable	γ	p Value
θ_1	9.51×10^{-5}	9.92×10^{-5}
θ_2	-4.90×10^{-5}	0.0782
θ_3	9.87×10^{-5}	0.5492
θ_4	-3.22×10^{-4}	4.09×10^{-40}

the convergence of the Pareto front over the four performed iterations. The top graph of Figure 10 shows the progression from the first iteration Pareto front (dashed black line) to the second iteration Pareto front (red line) along with the 11 selected alternatives (blue crosses) which were simulated (red circles) in order to obtain the

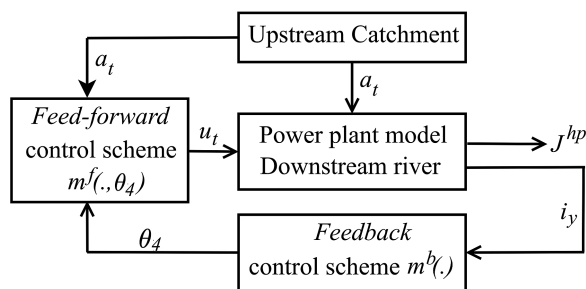


Figure 7. Scheme B—Mixed feedforward and feedback control.

second iteration front. Analogously the bottom graph in Figure 10 shows the progression from the third to the fourth iteration front. Once again the arrows help visualizing the differences e^j between the approximated objectives (J^{hp} and J^{inc}) and the simulated ones (J^{hp} and J^{inc}) for the selected alternatives at each iteration. The termination criteria is satisfied at the fourth iteration thus terminating the procedure (see Table 6).

Figure 11 compares the Pareto fronts determined with Schemes A and B. It is apparent that Scheme B dominates Scheme A. In particular:

1. Stopping the incision would cost € 2.5 million per year due to the consequent reduction in the hydro-power revenue (about 7.3% of the current yearly production) when adopting Scheme A, but only € 0.8 million per year (about 2.6% of current yearly production) when adopting Scheme B.
2. Halving the current rate of incision in the reach downstream from Cremona would cost € 0.5 million per year (about 1.5% of current yearly production) with Scheme A and only € 0.2 million with Scheme B (0.6% of current yearly production).

In addition, Scheme A does not allow to achieve any aggradation in the riverbed in order to restore previous degradation. This is possible with Scheme B: an aggradation of 2 cm/yr would cost € 1.6 million (about 5% of current yearly production).

Scheme B is conceptually more advanced than Scheme A. It provides an *online control* of the riverbed variation. The performances of Scheme A depends on the hydrological series used to run the optimization. In a context of fast changing flood occurrences its operating rules may result not so effective. The feed-back control of Scheme B is more resilient with this respect since the operating rule adapts itself to the new discharge inputs every year.

8. Discussion

The RSM provided a flexible approach to solving the design problem. This paper showed the potential of RSM which was previously applied to integrate a number of complex processes into WRM [Castelletti et al., 2010a] to embed fluvial geomorphological processes into WRM. Hence, a topic is addressed, and solved

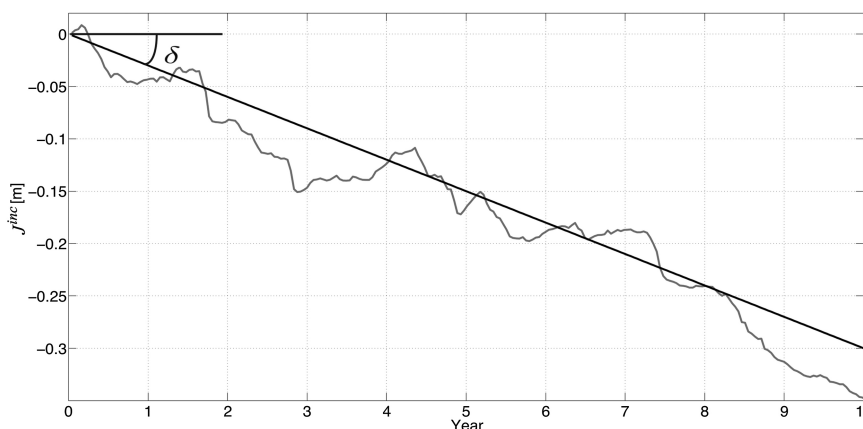


Figure 8. Control of morphological evolution: actual (gray, curve line) and targeted (black, straight line) trajectories of the incision (experiment with $\alpha=3700, \beta=4000, \delta=-0.03$ in equation (16)).

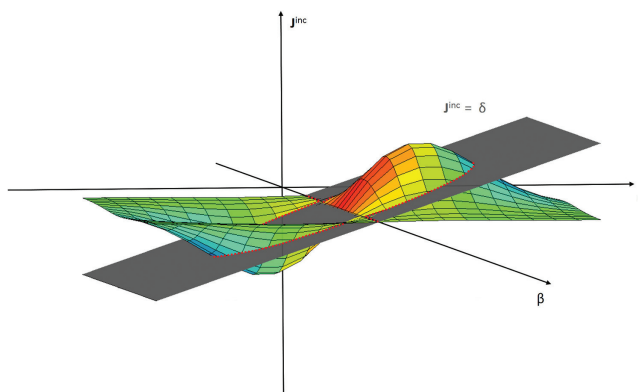


Figure 9. An exemplification of the surface J^{inc} in the 3-D space δ , β , and J^{inc} . The effective alternatives are the intersection points between the plane $J^{inc} = \delta$ and the J^{inc} .

here from a quantitative WRM perspective that was so far mainly acknowledged in qualitative terms [Petts and Gurnell, 2005].

The proposed case study of Isola Serafini is used as an illustrative example to introduce the general methodological framework. The model is applicable to other case studies if a hydro-morphological model with mobile boundaries, i.e., capable of simulating channel adjustment processes is available. This refers also to access to the detailed, morphologic data (cross sections) required for

model setup. The subsequent implementation of the response-surface is, in contrast, readily feasible with standard tools.

To implement the framework on other real-world applications is necessary to strength our capacity to assess the uncertainty associated with the pareto-optimal solutions derived. There are a number of hypothesis in the current implementation of the method that are case study sensitive and should be carefully checked for real applications.

In terms of hydromorphological assumptions we assumed complete sediment connectivity when all gates are opened. This hypothesis produced results in line with previous works focusing on sediment transport and management scenarios on the River Po [Schippa et al., 2006]. For real application it should be supported by field evidences as this hypothesis is likely to change significantly in function of the dam infrastructures installed.

Regarding the RSM methodology specifically two parameters need to be carefully tuned: (i) the threshold for the termination test in the LP-RS procedure, (ii) the number of alternatives along the Pareto front selected for PB hydro-morphological simulations at each iteration. The number of selected alternatives to be simulated could be denser at neuralgic points where conflicts are more severe and hence of higher interest for management, for instance. At the moment, there is no established procedure to measure the quality of the Pareto front through the LP-RS procedure [Castelletti et al., 2012] since the full Pareto front is not known. In general, reaching higher accuracy would lead to higher computational costs, which would nevertheless still be lower than direct integration of a hydro-morphological model into the optimization process.

The resulting Pareto front is an effective tool to inform decision makers with quantitative data [Castelletti et al., 2007, 2010a, 2012]. Increasing or decreasing the hydropower plant production has a significant effect on riverbed evolution and the trade-off between the two issues is fully appreciable (see Figure 11). The proposed procedure provides valuable information to negotiate operating rules and subsidiary measures, which is nowadays a request of water resource related legislation, such as the European Water Framework Directive [EU Water Framework Directive, 2000], which establishes that a specific operating rule should be implemented only if countermeasures to tackle the degradation of the fluvial system are planned and undertaken.

In the case of IS scheme B could be easily implemented since it requires only to change yearly the discharge level at which all gates are fully opened for flood pass-through. A monitoring system could be set up on the

river reach around Cremona to measure how the model prediction differ from the real channel process and if needed a recalibration of the model could be undertaken supported by field evidences. If successful, the new operating rule will help stabilizing

Parameter	Range	Step	\mathcal{N}_i
α	1200–4000	100	29
β	1000–7000	100	61
δ	–0.06–0.06	0.01	13

Table 6. Scheme B—Termination Test: The Average Distances \bar{e}^j Are Compared to the Thresholds λ^j (6% of the Ranges R^j)

j^i	Second Iteration			Third Iteration			Fourth Iteration		
	R^j	λ^j	\bar{e}^j	R^j	λ^j	\bar{e}^j	R^j	λ^j	\bar{e}^j
j^{hp} (10^6 €/yr)	1.8763	0.1126	0.1457	3.4226	0.2054	0.3587	3.4383	0.2063	0.1317
j^{inc} (m/yr)	0.0900	0.0054	0.0092	0.1200	0.0072	0.0147	0.1300	0.0078	0.0076

river infrastructures, limiting maintenance needs of navigation facilities and so counterbalancing the loss in hydropower revenue.

9. Conclusion

River geomorphology has become a key aspect of river management over the last years [Brierley et al., 2013]. However, the economical appraisal of direct and indirect ecosystem services affected by fluvial geomorphology is difficult to estimate [Newson and Large, 2006]. Fluvial geomorphic processes influence a variety of ecosystem services like water supply (since groundwater levels can relate to riverbed level), freshwater ecosystem integrity and flood mitigation (by destabilizing river infrastructures and reshaping channel forms) [Ausseil et al., 2013]. For this reason the integration of river geomorphology into water resource management is receiving growing attention [Yin et al., 2014; Wild and Loucks, 2014]. In this paper we provided a procedure to design optimal operating rules for a run-of-river power plant, which besides maximizing the energy production, reduce the riverbed incision rate downstream from the plant. To our knowledge, this is the first attempt to consider fluvial channel processes in designing operating rules from a MO perspective.

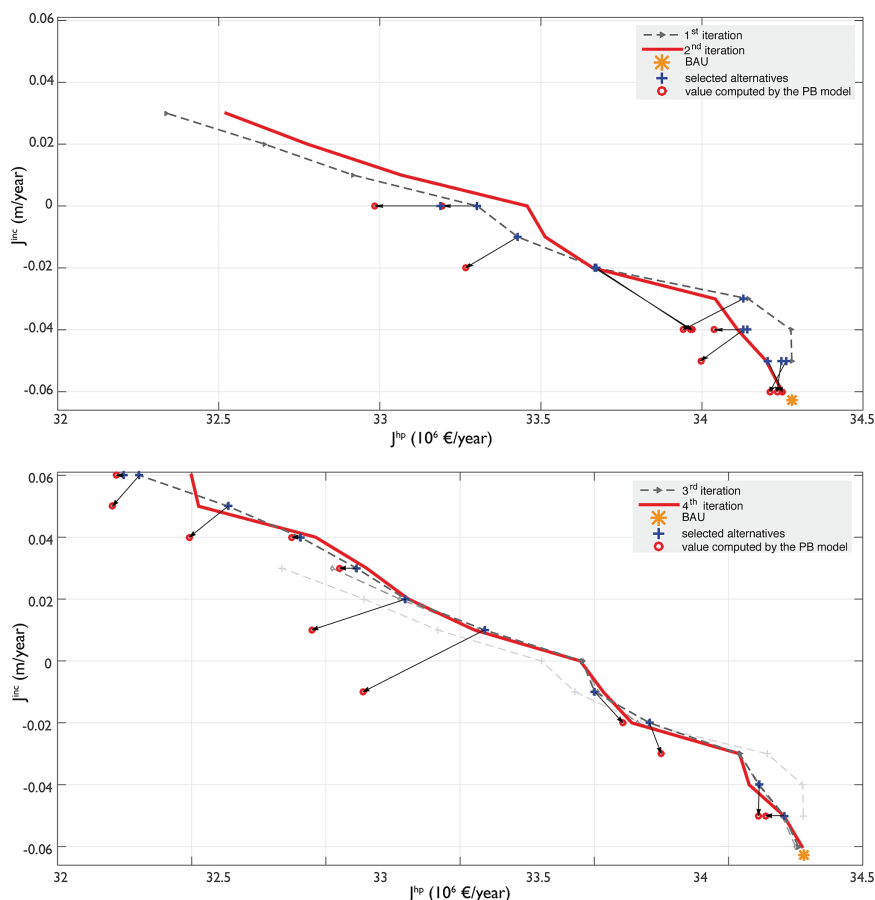


Figure 10. Scheme B—Pareto fronts at first and second iteration on the top graph and third and fourth iteration on the bottom graph. Blue crosses are alternatives selected on the first Pareto front (top graph) and third Pareto front (bottom graph), red dots are the values computed by the hydro-morphological model for those selected alternatives, and the yellow star is the BAU alternative.

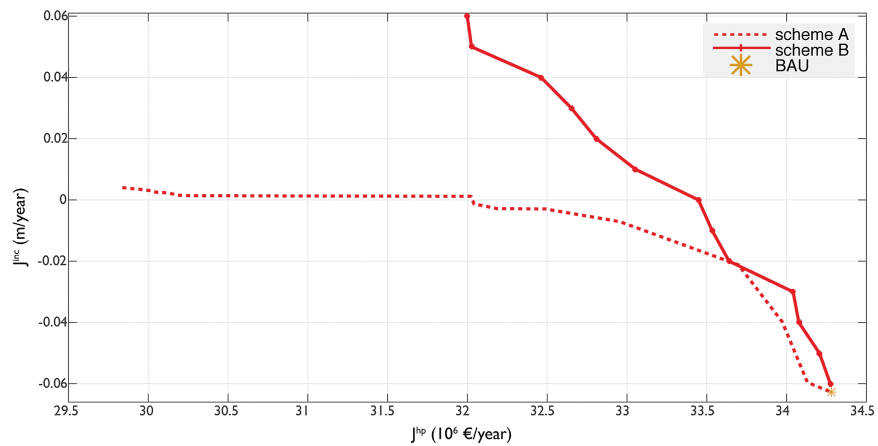


Figure 11. Comparison of Pareto fronts between Scheme A and Scheme B.

To achieve this aim, we propose a framework that adopts the RSM a surrogate modeling approach to include PB hydro-morphological modeling into an optimization procedure. Hence, this framework overcomes the high computational costs that so far hindered the integration of river morphology into WRM. We provided numerical proof that river morphologic processes and hydropower production are indeed in conflict, but that the conflict can be mitigated with appropriate control strategies.

Nowadays, various models exist to reproduce river channel processes from reach to catchment scales [Brasington and Richards, 2007]. This paper shows some currently unexplored potentials of coupling these advances with state of art in surrogate modeling [Castelletti et al., 2012; Razavi et al., 2012] to integrate more effectively fluvial geomorphology understanding into water resources management: a necessity no longer negligible.

Appendix A: Learning and Planning Response Surface Procedure

The Learning and Planning RS (LP-RS) procedure is a version of the RSM proposed by Castelletti et al. [2010a] for solving the MO Design Problem using a Global Interactive Response Surface Method. It consists of four iterative steps plus an initialization (Design of Experiment (DOE)) and a termination test (see Figure 12) [Castelletti et al., 2010a, 2010b].

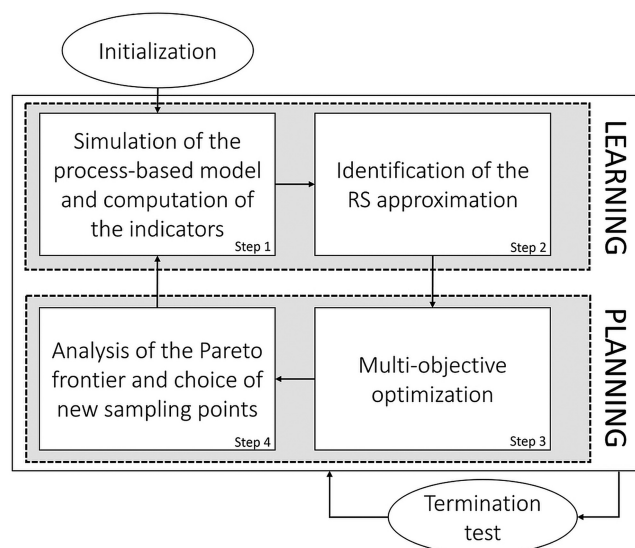


Figure 12. The iterative learning and planning procedure based on RSM [Castelletti et al., 2010a].

In the first step (see Figure 12), at the k th iteration ($k = 1, 2, \dots$) of the procedure, N_k simulations of the PB model (see equation (13b)) are run, in correspondence of N_k different instantiations $\theta_1, \dots, \theta_{N_k}$ of the parameter θ and, for each instantiation, say the j th one, the corresponding value $J(\theta_j)$ is computed.

In the second step, the N_k couples $(\theta_j, J(\theta_j))$ are used to identify, via interpolation, an approximation $\hat{J}^k(\cdot)$ of the (unknown) RS $J(\cdot)$.

In the third step, the following MO design problem, based on the approximated RS, is solved:

$$\min_{\theta \in \Theta} \hat{J}^k(\theta), \quad (A1)$$

and its Pareto front determined. If the number of considered alternatives is relatively small, as in our case, the optimization can be performed exhaustively i.e., comparing each alternative with all the others to identify the Pareto efficient ones.

In the fourth step, this Pareto front is analyzed and N_{k+1} interesting points $\hat{J}_1, \dots, \hat{J}_{N_{k+1}}$ are selected. The corresponding points $\theta_1, \dots, \theta_{N_{k+1}}$ in the parameter space constitute the new sample of the parameter θ that will be simulated at Step 1 of the subsequent iteration.

The Initialization step (Design Of Experiments DOE) requires to choose the first N_1 instantiations $\theta_1, \dots, \theta_{N_1}$ to be simulated at the first iteration ($k = 1$). The DOE must effectively sample the decision space and can be based either on statistical techniques [e.g., Kleijnen, 2008], and references therein] or on the basis of physical considerations and a priori knowledge [Castelletti et al., 2010a, 2010c]. Starting from the second iteration, the termination test is performed as described in the text.

Acknowledgments

The authors wish to thank Sara Pavan at AIPO (www.agenziainterregionalepo.it, Interregional Agency for Po River Management) for the early development and setting of the numerical model. River Po cross sections surveys have been kindly provided by AIPO. Flow data about Po River daily average flow rates and stage-discharge rating curves at several stations are freely available on ARPA website (www.arpa.emr.it, Emilia Romagna Environment Protection Agency). The authors also thank Rafael Schmitt for his precious comments. Finally, we thank the unanimous reviewers of the paper which helped us to improve the quality of the paper with their relevant comments.

References

- Ausseil, A., J. R. Dymond, M. U. F. Kirschbaum, R. M. Andrew, and R. L. Parfitt (2013), Assessment of multiple ecosystem services in New Zealand at the catchment scale, *Environ. Modell. Software*, *43*, 37–48, doi:10.1016/j.envsoft.2013.01.006.
- Bernardi, D., S. Bizzi, S. Denaro, Q. Dinh, S. Pavan, L. Schippa, and R. Soncini-Sessa (2013), Integrating mobile bed numerical modelling into reservoir planning operations: The case study of the hydroelectric plant in Isola Serafini (Italy), in *WIT Transactions on Ecology and the Environment*, vol. 178, edited by C. A. Brebbia, 13 pp., WIT Press, Southampton, U. K., doi:10.2495/WS130061.
- Bonomo, F., and C. Luisa (2011), La nuova conca di Isola Serafini, Cemento Calcestruzzo, 105–115, Novembre 2011, Edizione PEI, Parma. [Available at http://www.edizionipei.it/uscite_riviste-quarry_and_construction-novembre_2011.html.]
- Box, G. E., and K. Wilson (1951), On the experimental attainment of optimum conditions, *J. R. Stat. Soc., Ser. B*, *13*(1), 1–45.
- Brasington, J., and K. Richards (2007), Reduced-complexity, physically-based geomorphological modelling for catchment and river management, *Geomorphology*, *90*(3–4), 171–177, doi:10.1016/j.geomorph.2006.10.028.
- Brierley, G., K. Fryirs, C. Cullum, M. Tadaki, H. Q. Huang, and B. Blue (2013), Reading the landscape: Integrating the theory and practice of geomorphology to develop place-based understandings of river systems, *Prog. Phys. Geogr.*, *37*(5), 601–621, doi:10.1177/0309133313490007.
- Burke, M., K. Jorde, and J. M. Buffington (2009), Application of a hierarchical framework for assessing environmental impacts of dam operation: Changes in streamflow, bed mobility and recruitment of riparian trees in a western North American river, *J. Environ. Manage.*, *90*, suppl. 3, S224–S236.
- Capart, H., T. Eldho, S. Huang, D. Young, and Y. Zech (2003), Treatment of natural geometry in finite volume river flow computations, *J. Hydraul. Eng.*, *129*(5), 385–393, doi:10.1061/(ASCE)0733-9429(2003)129:5(385).
- Castelletti, A., F. Pianosi, and R. Soncini-Sessa (2007), Integration, participation and optimal control in water resources planning and management, *Appl. Math. Comput.*, *206*(1), 21–33, doi:10.1016/j.amc.2007.09.069.
- Castelletti, A., F. Pianosi, R. Soncini-Sessa, and J. P. Antenucci (2010a), A multiobjective response surface approach for improved water quality planning in lakes and reservoirs, *Water Resour. Res.*, *46*, W06502, doi:10.1029/2009WR008389.
- Castelletti, A., A. Lotov, and R. Soncini-Sessa (2010b), Visualization-based multi-objective improvement of environmental decision-making using linearization of response surfaces, *Environ. Modell. Software*, *25*(12), 1552–1564.
- Castelletti, A., S. Galelli, M. Restelli, and R. Soncini-Sessa (2010c), Tree-based reinforcement learning for optimal water reservoir operation, *Water Resour. Res.*, *46*, W09507, doi:10.1029/2009WR008898.
- Castelletti, A., S. Galelli, M. Ratto, R. Soncini-Sessa, and P. Young (2012), A general framework for dynamic emulation modelling in environmental problems, *Environ. Modell. Software*, *34*, 5–18, doi:10.1016/j.envsoft.2012.01.002.
- Dittmann, R., F. Froehlich, R. Pohl, and M. Ostrowski (2009), Optimum multi-objective reservoir operation with emphasis on flood control and ecology, *Nat. Hazards Earth Syst. Sci.*, *9*(6), 1973–1980.
- Engelund, F., and E. Hansen (1967), *A Monograph on Sediment Transport in Alluvial Streams*, Teknisk Forlag, Copenhagen.
- EU Water Framework Directive (2000), Directive 2000/60/ec of the European Parliament and of the council: Establishing a framework for community action in the field of water policy, *Off. J. Eur. Communities*, *L327*, 1–71.
- Gómez, C. M., C. D. Pérez-Blanco, and R. J. Batalla (2013), Tradeoffs in river restoration: Flushing flows vs. hydropower generation in the Lower Ebro River, Spain, *J. Hydrol.*, *518*, 130–139, doi:10.1016/j.jhydrol.2013.08.029.
- Grant, G. E., J. C. Schmidt, and S. L. Lewis (2003), A geological framework for interpreting downstream effects of dams on rivers, in *A Peculiar River*, *Water Sci. Appl.*, edited by J. E. O'Connor and G. E. Grant, pp. 209–226, AGU, Washington, D. C., doi:10.1029/007WS13.
- Gupta, H., S.-J. Kao, and M. Dai (2012), The role of mega dams in reducing sediment fluxes: A case study of large Asian rivers, *J. Hydrol.*, *464–465*, 447–458.

- Kleijnen, J. P. (2008), Response surface methodology for constrained simulation optimization: An overview, *Simul. Modell. Pract. Theory*, 16(1), 50–64.
- Kohavi, R., et al. (1995), A study of cross-validation and bootstrap for accuracy estimation and model selection, in *Proceedings of the 14th International Joint Conference on Artificial Intelligence*, vol. 14, pp. 1137–1145, Morgan Kaufmann, San Francisco, Calif.
- Kondolf, G. M. (1997), Hungry water: Effects of dams and gravel mining on river channels, *Environ. Manage.*, 21(4), 533–551.
- Langendoen, E. J., R. R. Wells, R. E. Thomas, A. Simon, and R. L. Bingner (2009), Modeling the evolution of incised streams III: Model application, *J. Hydraul. Eng.*, 135(6), 476–486.
- Lotov, A. V., V. A. Bushenkov, and G. K. Kamenev (2004), *Interactive Decision Maps: Approximation and Visualization of Pareto Frontier*, vol. 89, Kluwer Acad., Boston, Mass.
- Magilligan, F. J., and K. H. Nislow (2005), Changes in hydrologic regime by dams, *Geomorphology*, 71(1), 61–78.
- Manning, R. (1891), On the flow of water in open channels and pipes, *Trans. Inst. Civ. Eng. Ireland*, 20, 161–207.
- Ministero delle Politiche Agricole Alimentari e Forestali (1990), *Po Acquagricolturambiente: l'alveo e il delta*, vol. 2, pp. 184–195, Il Mulino, Bologna.
- Newson, M. D., and A. R. G. Large (2006), “Natural” rivers, “hydromorphological quality” and river restoration: A challenging new agenda for applied fluvial geomorphology, *Earth Surf. Processes Landforms*, 31, 1606–1624.
- Nicklow, J., and L. Mays (2000), Optimization of multiple reservoir networks for sedimentation control, *J. Hydraul. Eng.*, 126(4), 232–242, doi:10.1061/(ASCE)0733-9429(2000)126:4(232).
- Nicklow, J. W., and O. Ozkurt (2003), Control of channel bed morphology in large-scale river networks using a genetic algorithm, *Water Resour. Manage.*, 17(2), 113–132.
- Park, J.-S. (1994), Optimal latin-hypercube designs for computer experiments, *J. Stat. Plann. Inference*, 39(1), 95–111.
- Petts, G. E., and A. M. Gurnell (2005), Dams and geomorphology: Research progress and future directions, *Geomorphology*, 71(1), 27–47.
- Poff, N. L., and D. D. Hart (2002), How dams vary and why it matters for the emerging science of dam removal, *Bioscience*, 52(8), 659–668, doi:10.1641/0006-3568(2002)052[0659:HDVAWI]2.0.CO;2.
- Razavi, S., B. A. Tolson, and D. H. Burn (2012), Review of surrogate modeling in water resources, *Water Resour. Res.*, 48, W07401, doi:10.1029/2011WR011527.
- Rosatti, G., A. Armanini, V. Galletta, M. Vergnani, and F. Cerchia (2008), *L'uso dei Pennelli per la Riduzione Della Barra Forzata in Prossimità del Punto di Inflexione tra due Curve Susseguenti: Uno Studio Numerico Relativo al po*, pp. 151–151, Atti del convegno 31° Convegno Nazionale di Idraulica e Costruzioni Idrauliche, Perugia, 9–12 Settembre 2008.
- Schippa, L., and S. Pavan (2008), Analytical treatment of source terms for complex channel geometry, *J. Hydraul. Res.*, 46(2), 753–763, doi:10.1080/00221686.2008.9521920.
- Schippa, L., and S. Pavan (2009), Bed evolution numerical model for rapidly varying flow in natural streams, *Comput. Geosci.*, 35(2), 390–402.
- Schippa, L., S. Pavan, and S. Colonna (2006), River Po low water training. The importance of mathematical modelling to support designing activities, in *River Flow 2006*, vol. 2, edited by R. M. L. Ferreire, E. C. T. L. Alves, and J. G. A. B. Leal, pp. 1973–1983, London, U. K.
- Soncini-Sessa, R., E. Weber, and A. Castelletti (2007), *Integrated and Participatory Water Resources Management: Theory*, vol. 1, Elsevier Sci., Amsterdam, Netherlands.
- Surian, N., and M. Rinaldi (2003), Morphological response to river engineering and management in alluvial channels in Italy, *Geomorphology*, 50(4), 307–326.
- Tang, B. (1993), Orthogonal array-based latin hypercubes, *J. Am. Stat. Assoc.*, 88(424), 1392–1397.
- Wang, G. G., Z. Dong, and P. Aitchison (2001), Adaptive response surface method—A global optimization scheme for approximation-based design problems, *Eng. Opt.*, 33(6), 707–734.
- Wild, T. B., and D. P. Loucks (2014), Managing flow, sediment, and hydropower regimes in the Sre Pok, Se San, and Se Kong Rivers of the Mekong basin, *Water Resour. Res.*, 50, 5141–5157, doi:10.1002/2014WR015457.
- Wu, F.-C., and Y.-J. Chou (2004), Tradeoffs associated with sediment-maintenance flushing flows: A simulation approach to exploring non-inferior options, *River Res. Appl.*, 20(5), 591–604, doi:10.1002/rra.783.
- Yin, X., Z. Yang, W. Yang, Y. Zhao, and H. Chen (2009), Optimized reservoir operation to balance human and riverine ecosystem needs: Model development, and a case study for the Tanghe reservoir, Tang river basin, China, *Hydrol. Processes*, 24(4), 461–471, doi:10.1002/hyp.7498.
- Yin, X.-A., Z.-F. Yang, G. E. Petts, and G. M. Kondolf (2014), A reservoir operating method for riverine ecosystem protection, reservoir sedimentation control and water supply, *J. Hydrol.*, 512, 379–387, doi:10.1016/j.jhydrol.2014.02.037.